Sci., J.Fac., Sci., Minufiya Univ., 2005 Vol. XIX, 1 - 32

FACIES ANALYSIS OF THE CENOMANIAN-TURONIAN SUCCESSION AT GABAL SHABRAWET AND GABAL ATAQA, GULF OF SUEZ REGION, EGYPT: IMPLICATION FOR RECONSTRUCTION OF RELATIVE SEA LEVEL CHANGES

Mohamed M. Abu El-Hassan[1] and Ryuji Tada[2]
1 Geology Department, Faculty of Science, Menoufia University, Shebin El-Kom Egypt
2 Department of Earth and Planetary Science, The University of Tokyo, 7-3-1Hongo , Bunkyo-ku, Tokyo 113-0033, Japan,

ABSTRACT

Cenomanian-Turonian siliciclastic-carbonate strata that exposed at Gabal Ataqa and Gabal Shabrawet, along the western side of the Suez Gulf are classified into nine lithologic units. These lithofacies are mainly shallow marine carbonate sediments of supratidal to subtidal deposition. Two main types of erosional surfaces are identified: 1) subaerial erosional surface (SES) at the Cenomanian/Turonian boundary (C/T), and 2) ravinement surfaces (RvS) at the Early-Middle Cenomanian.

The depositional depth across C/T is well represented. The relative sea level changes in the studied areas is represented by sea level rise during Early to Middle Cenomanian and moderate fall of sea level at the end of Middle Cenomanian. Sea level changes during the Late Cenomanian is characterized by 1) gradual rise of sea level during the early Late Cenomanian, 2) gradual fall of sea level with high frequency oscillations during the middle Late Cenonmanian, 3) gradual rise of sea level at the late Late Cenomanian, and 4) abrupt regression with large sea level drop at C/T boundary. The sea level changes during Turonian is characterized by 1) lowstand of sea level during the Early Turonian, 2) fall of sea level in the Middle Turonian, and 3) rapid sea level rise at the beginning of Late Turonian is also obvious. The trend of reconstructed sea level changes in Egypt generally agrees with the previously reported reconstructions. However, our reconstruction is with higher time resolution and revealed the presence of higher frequency sea level oscillations during the middle Late Cenomanian.

Keywords: Cenomanian-Turonian, Gulf of Suez, microfacies, Egypt

INTRODUCTION

Late Cenomanian to Early Turonian is a period of major biotic and oceanic changes. The Cenomanian-Turonian boundary in North American and European sections are characterized by deposition of black shales and a positive excursion in $\delta^{13}C$ (Schlanger and Jenkyns, 1976; Jenkyns, 1980; and Arthur et al., 1987). The positive $\delta^{13}C$ excursion is also recognized worldwide (Jarvis et al., 1988; Hart et al., 1991, and Gate et al., 1993).

Flexer et al. (1986) reconstructed relative sea level changes during the Cretaceous in Israel. They reported that the sea level dropped during the latest Cenomanian (near the Cenomanian-Turonian boundary) with renewed transgression during the Early Turonian. They concluded that the conspicuous lowstand and faunal break at the Cenomanian-Turonian boundary in Israel may be local. Bogoch et al. (1993) described calcrete crusts from the top of the Sakhnin Formation (Late Cenomanian) in North Israel and concluded that the Cenomanian/Turonian boundary represents a drop in sea level manifested by subaerial exposure. Similar sea level drop at the C/T boundary is reported from the British Chalk (Hancock, 1989). On the other hand, Weimer (1984) studied the relation of unconformities with tectonic sea level changes during the Cretaceous in the Western Interior, U.S.A. He reported a faunal break at the Middle Turonian at (90 Ma.) with drop of sea level.

In Egypt, the transgression of Tethys started during the early Cretaceous and continued during the Late Cretaceous, which extended to the Sudan-Egypt border (Said, 1990 and Issawi et al., 1999). Issawi et al. (1994) studied the depositional environments of the Cenomanian-Turonian sequences in Sinai and Gulf of Suez areas based on the variation in sediments and fossil assemblages. They remarked shallow conditions during Early-Middle Cenomanian, gradual deep marine conditions (rise sea level with oscillations) during Late Cenomanian. They remarked shallower conditions during the Early Turonian, regressive phase drop during the Middle Turonian and more deep marine conditions during Late Turonian in Sinai. Darwish (1994) studied the Cenomanian-Turonian sequence stratigraphy of northern Egypt. He detected unconformities and diastems in Late Albian-Early Cenomanian, intra-middle Cenomanian and Middle-Late Turonian with maximum sea level rise and landmass imundation during Late Turonian. Recently Bauer et al. (2001) recorded the major hiatus at trhe Cenomanian/Turonian boundary at Sinai, Egypt. They argued

the Cenomanian/Turonian hiatus in Sinai to initial intracratonic compression associated with Syrian Arc tectonics.

In the present work, the exact position and nature of Cenomanian-Turonian boundary (C/T) is not well understood especially with respect to relative sea level changes in the studied area. The present study is focused on establishing detailed stratigraphy of the Cenomanian-Turonian, and reconstructing the relative sea level changes at Gabal Shabrawet and Ataqa along the Gulf of Suez in order to **1)** specify the exact position of the C/T boundary, **2)** specify the erosional surfaces within the Cenomanian-Turonian succession, **3)** reconstruct the relative sea level curve in the studied areas during the Cenomanian-Turonian deposition, and **4)** the origin of red beds at C/T boundary.

GEOLOGICAL SETTING

Gabal Shabrawet and Gabal Ataqa are located in the northern part of the Eastern Desert along the Gulf of Suez (Fig. 1). The Cretaceous successions in Shabrawet area remarked at Shabrawet Proper and Shabrawet West (Al-Ahwani, 1982). The Shabrawet Proper and West are characterized by steeply dipping Cretaceous strata, which is surrounded by gently dipping Eocene and younger strata (Fig. 2) and consists of douple punging anticline with plunging axes NE-SW direction. The core of the anticline represented by Aptian-Albian siliciclastic-carbonate deltaic sediments. The major faults trend is 60° NE in the studied area.

Gabal Ataqa stands as a prominent mountain on the junction between the Gulf of Suez and the Suez Canal. It lies 70 km to the southeast of Gabal Shabrawet. GabalAtaqa is a tilted fault block, sloping towards the southwest with a dip of beds up to 85°. This block is bounded by NE-SW trending normal faults with generally northeastward dips. A clear outcrop of Cenomanian-Turonian succession is presented in the southeastern corner of Gabal Ataqa, which is dissected by a major fault running in a NE-SW direction (El-Akkad and Abdallah, 1971). Late Cretaceous orogenic movements resulted in folding and faulting of the Cretaceous sequences in Shabrawet and Ataqa areas. This orogeny coincides with the Laramide movements of the Syrian Arc movements in north Egypt, which extended from Syria through Lebanon and north Sinai to the Western Desert of Egypt (Al-Ahwani, 1982).

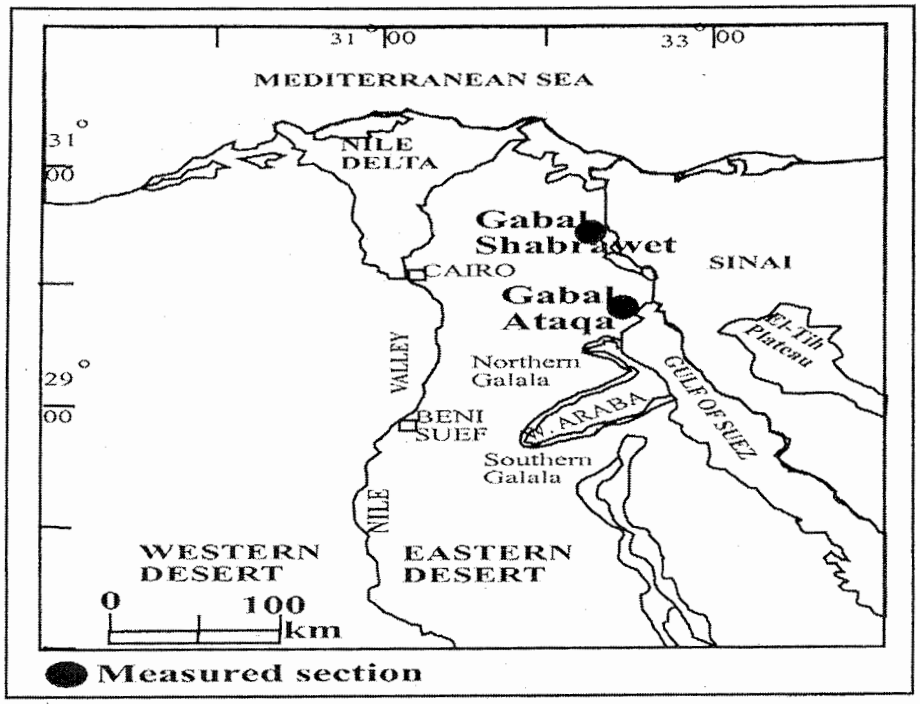

Fig. (1): Location map of the studied areas at Gabal Shabrawet and Gabal Ataqa along the western side of Gulf of Suez (Geological map of Egypt, EGSMA, 1981).

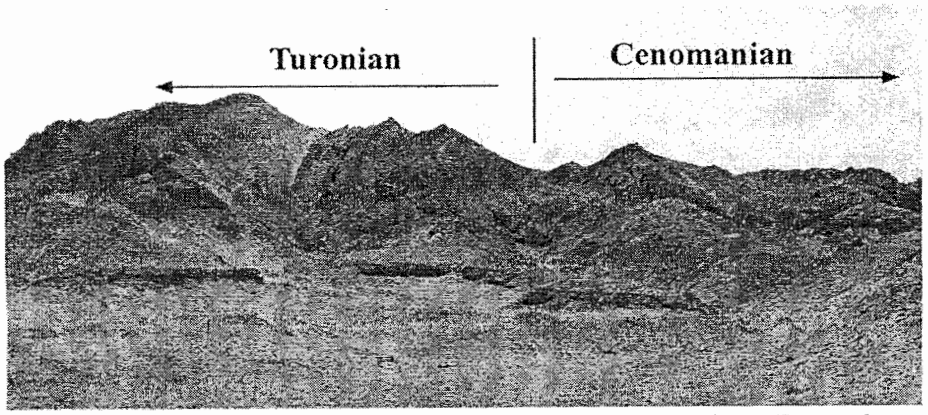

Fig. (2): Panoramic view shows the Cenomanian-Turonian succession at Gabal Shabrawet Proper, Ismailia-Suez District.

METHODOLOGY

Approximately 200 samples were collected from the Cenomanian and Turonian sequences at Gabal Shabrawet and Gabal Ataqa. These samples were subjected to petrographical, mineralogical, and chemical analyses in order to examine the composition of rocks and sedimentary textures. Thin sections were made for 70 samples selected to represent different rock types. The mineralogical analyses were carried out on 60 selected bulk carbonate samples to characterize the limestone and dolomite rock types. Powdered sample mounted on a glass holder is X-rayed from 2 to 60° with a scanning speed of 2θ/min. by a MAC Science MXP-3 X-ray diffractometer equipped with a CuKα tube and monochrometer. Separation of the clay fraction (<2mm) was carried out on shale samples to examine the clay mineral composition. Chemical scanning of slab samples were conducted using "Horiba" X-ray microscope XGT-2700. XGT is the XRF scanner capable of quantitatively measurements of major elements in the mineral. All methods are carried out at the Department of Earth and Planetary Sciences (EPS), the University of Tokyo.

LITHOSTRATIGRAPHY

The exact position and nature of the Cenomanian-Turonian boundary at Gabal Shabrawet and Gabal Ataqa focused on the detailed description of lithological characters, erosional surfaces, and fossil occurrences of the Cenomanian-Turonian strata at Gabal Shabrawet and Gabal Ataqa. The Cenomanian succession in these areas is named Galala Formation of El Akkad and Abdallah, (1971), which is 90-120 m thick being subdivided into lower, middle, and upper members based on lithology and fossil occurrences.

The Cenomanian Galala Formation at Gabal Shabrawet unconformably overlies the Aptian-Albian siliciclastic-carbonate rocks of the Risan Aneiza Formation. It attains a thickness reaching to 90 m and generally consists of dolostone, dolomitic limestone, marl, and bioturbated medium to coarse graine siliciclastic sandstone (Fig. 3). At Gabal Shabrawet, the lower member of Galala Formation consists of white, moderately massive limestone and pale yellow, massive clayey to sandy dolostone. The middle member consists of alternations of white to yellow, massive hard limestone, yellowish brown moderately hard marlstone, and yellow clayey dolostone. The upper member consists of yellowish to reddish white dolostone and yellow clayey dolostone intercalated with thin beds of siliciclastic sandstone. At Gabal Ataqa, the lower member of the Galala Formation is composed of yellowish bioturbated sandy dolostone

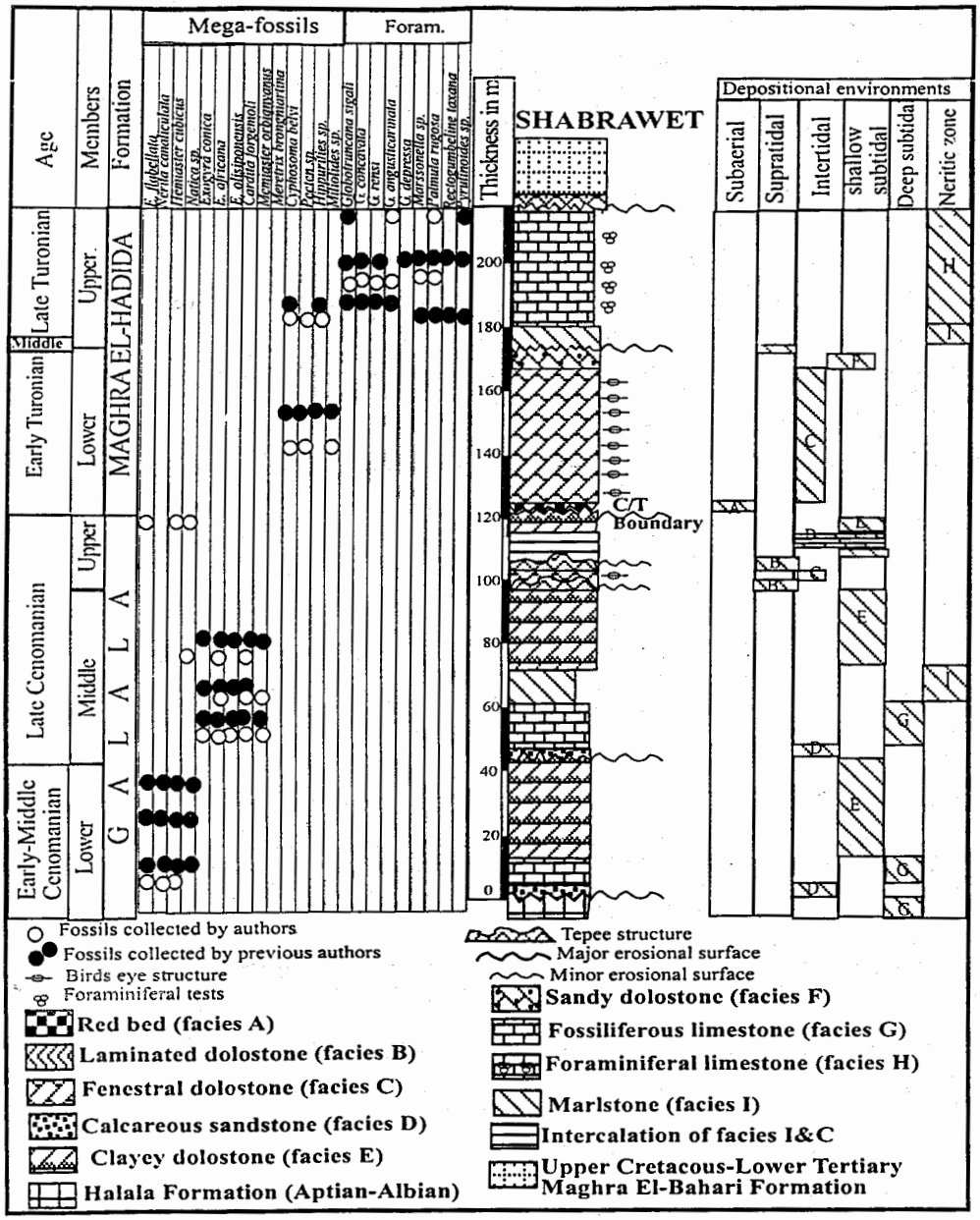

Fig. (3): Litho- and bio-stratigraphy and depositional environments of the Cenomanian-Turonian succession at Gabal Shabrawet.

Table (1): Correlation of the Cenomanian-Turonian formations in the studied areas, Sinai and Israel.

Localities / Age	The present study		Sinai		Israel Southern Negev Lewy, (1996)	
	Gabal Shabrawet	Gabal Ataqa	North (Abdel-Gawad, 1999 & Issawi, et al. 1999)	Central (Abdel-Gawad, 1999 & Issawi, et al. 1999)		
Turonian	Maghra El-Hadida		Wata	Wata	Gerofit	Judea Group
			Butum	Butum		
			Abu Qada	Abu Qada	Ora Shale	
Cenomanian	Galala		Galala / Halal	Raha	Hazera	

intercalated with gray to greenish gray fine silty claystone (Fig. 4). The middle member consists of yellowish marl intercalated with thin white limestone. The upper member is yellowish siliciclastic sandstone and hard massive clayey dolostone intercalated with few centimeters thick sandstone beds.

The Galala Formation is overlained by red ferruginous bed with erosional irregular contact. This red bed grades upward into the Maghra El-Hadida Formation (El-Akkad and Abdallah, 1971) with gradational contact at Gabal Shabrawet. This red bed extends 3-4 km laterally from Gabal Shabrawet Proper to Gabal Shabrawet West with its thickness ranges from 20 cm to 1 m (average 60 cm thick). The red bed is characterized by friable to moderately massive clays with rock fragments reworked from the underlying Galala Formation. The gradational contact of the red bed with the overlying Maghra El-Hadida Formation suggests that the red bed belongs to the Maghra El-Hadida Formation.

The Turonian succession was named Maghra El-Hadida Formation (El-Akkad and Abdallah, 1971). This formation is 120-140 m thick and was subdivided into two lower and upper members based on lithology and fossil occurrences. At Gabal Shabrawet and Gabal Ataqa, the lower member of the Maghra El-Hadida Formation overlies the red bed with gradational contact and is composed of white, massive, hard dolostone with bird's eye structures and topped by sandy dolostone facies (Figs. 3 and 4). At Gabal Ataqa, the lower member of the Turonian Maghra El-Hadida Formation underlies the upper member by non-fossiliferous sandstone with irregular erosional surface. This sandstone bed disappeared at Gabal Shabrawet but the iron nodules with thin crust of iron oxides occur instead of the sandstone bed above the lower member of the Maghra El-Hadida Formation with irregular erosional surface. The upper member at Gabal Shabrawet and Gabal Ataqa consists of yellow, massive, hard marlstone and white chalky limestone.

BIOSTRATIGRAPHY

The biostratigraphic analysis of the Cenomanian-Turonian succession at Gabal Ataqa and Gabal Shabrawet studied previously by many authors (El-Akkad and Abdallah,1971; Al-Ahwani, 1982; Abu Khadra et al., 1987; and Abdallah et al., (1988). Bivalves and echinoderms are diagnostic fossils to distinguish between the Cenomanian and Turonian succession. According to Al-Ahwani, (1982) and El-Akkad and Abdallah (1971) the following bivalves and echinoderms represent a Cenomanian age with different species assemblages between the lower, middle, and upper members of the Galala Formation at Gabal Shabrawet and Gabal

Ataqa. The lower member of the Galala Formation at Gabal Ataqa and Gabal Shabrawert is characterized by Cenomanian bivalves such as *Exogyra flabellate, Nerita canaliculata, Hemiaster cubicus*, and *Natica* sp. (Figs. 3 and 4). The middle member of the Galala Formation is characterized by *Exogyra conica, E. africana, E. olisiponensis, Hemiaster orbignyanus, Cardita forgemoli,* and *Meretrix brongniartina* (Figs. 3 &4). Al-Ahwani (1982) could not find any fossils in the upper member of the Galala Formation. In this study, the authors found *Natica* sp. and *Exogyra* sp, which suggest Cenomanian age (Abdallah et al. 1963), in the clayey dolostone lithofacies of the upper member with 2-3 m thick below the red bed at Gabal Shabrawet. Orabi (1994) identified the age diagnostic ostracodal species *Veeniacythereis jezzineensis, Cytherella cf. ovata, C. gigantosulcata,* and *N.bisulcata* in the lower member which suggest Early-Middle Cenomanian age, and *Planileberis pustulate, Looneyella sohni,* and *Bythocypris* sp in the middle and upper members of the Galala Formation at Gabal Ataqa, which suggest Late Cenomanian age (Fig. 4).

The bivalves and echinoidal fossils in the Turonian Maghra El-Hadida Formation were identified at Gabal Shabrawet and Gabal Ataqa. According to Al-Ahwani (1982), *Cyphosoma baylei, Pecten* sp. *Hippurites* sp. and *Miliolids* occurs in the lower member of the Maghra El-Hadida Formation. El-Akkad and Abdallah (1971) found ammonite *Pseudaspidoceras* (Solger) in the lower member, which indicate Early Turonian age. According to Al-Ahwani (1982), the upper member of the Maghra El-Hadida Formation contains abundant planktonic foraminifera *Globotruncana sigali, G. concavata, G. rensi, G. fornicata, G. imbricata, Globigerinelloides ehrenbergi,* and G. *asper*, and benthic foraminifera such as *Gyroidina girardana, G. depressa, pyrulinoides acuminata, Faujasina carinata,* and *Palmula rugosa* which are similar to the assemblage in the Upper Turonian Wata Formation in Central Sinai (Abdel-Gawad, 1999).

The Cenomanian-Turonian strata at Gabal Ataqa and Gabal Shabrawet are correlated with the strata in Sinai and Israel based on the fossil assemblages (Table 1). Orabi (1994) assigned the lower member of the Galala Formation to Early-Middle Cenomanian based on the ostracoda species *Veeniacythereis jezzineensis, Cytherella cf. ovata, C. gigantosulcata*, and *Neocythere.bisulcat* (Rosenfeld), and the middle and upper members to Late Cenomanian based on the ostacodal species such as *Planileberis pustulate, Looneyella sohni, Neocythere hevyonensis* (Rosenfeld), and *Bythocypris* sp. He also correlated these Early-Middle ostracodal assemblages of Galala Formation at Gebel Ataqa with those in

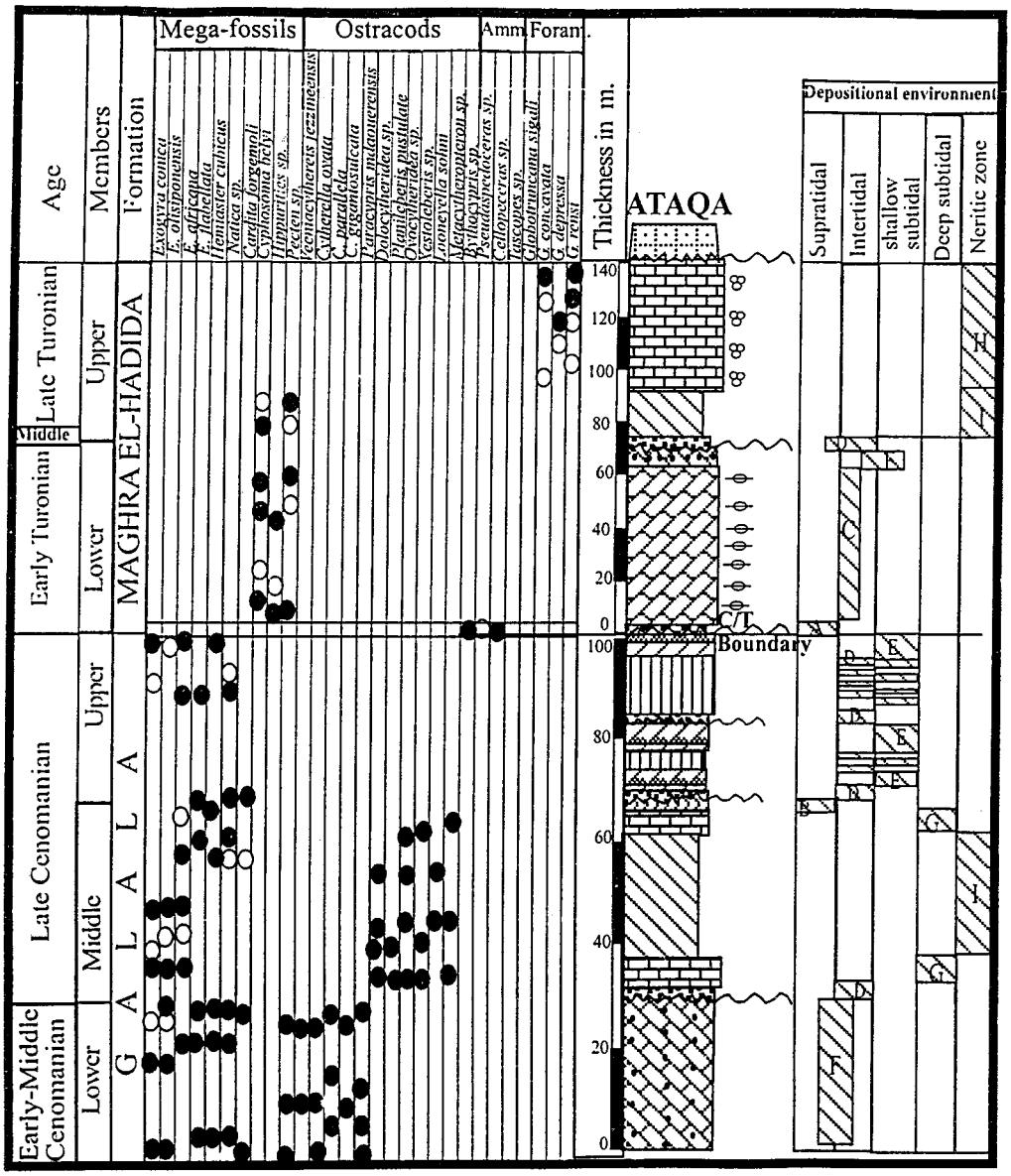

Fig. (4): Litho- and bio-stratigraphy and depositionalenvironments of the Cenomanian-Turonian succession at Gabal Ataqa.

Sinai and Israel (Honigstein et al., 1985). At Gabal Ataqa the Early Turonian is assigned based on the ammonite *Pseudaspidoceras* and *Choffaticeras segne* (El-Akkad and Abdallah, 1971 and personal communication of Prof. Dr. Tanabe, Universwity of Tokyo). Issawi et al. (1999) and Abdel-Gawad (1999) subdivided the Turonian sequence in Sinai into the lower, middle and upper parts based on ammonite and foraminifera. They assigned the lower part Abu Qada Formation in Sinai to Early Turonian based on the ammonite fossils and the middle part (the Butum Formation) to Middle Turonian and the upper part Wata Formation to Late Turonian. The Early Turonian Abu Qada Formation in Sinai is correlated to the lower member of the Maghra El-Hadida Formation at Gabal Ataqa based on the ammonite fossils (*Pseudaspidoceras)*. The Butum Formation in Sinai is red sandstone bed without fossils (Cherif et al., 1989). The Butum Formation overlies the Early Turonian (Abu Qada Formation) and underlies the Late Turonian (Wata Formation) by erosional surfaces in Negev, Israel, (Bartov and Steinitz, 1977) which are interpreted as regressive phase. This regressive phase (Butum Formation) is equivalent to the non-fossiliferous reddish yellow sandstone bed in the middle part of Maghra El-Hadida Formation of Gabal Ataqa (Issawi et al., 1999). Also, the Late Turonian Wata Formation in Sinai is equivalent to the upper member of Maghra El-Hadida Formation at Gabal Ataqa based on the assemblage of foraminiferal fossils of *Gyroidina girardana, G. depressa, pyrulinoides acuminata, Faujasina carinata.*

The Cenomanian-Turonian succession at Gabal Shabrawet and Gabal Ataqa contain faunal assemblages support the age control. The assemblage of ostracodal species in the Galala Formation at Gebel Ataqa is assigned to Early-Middle and Late Cenomanian based on the correlation with the similar ostracodal assemblages in Israel (Orabi, 1994; Rosenfeld and Raab, 1974 and Honigstein et al., 1985). The Abu Qada Formation in Egypt is assigned to Early Turonian based on the ammonite of *Pseudaspedoceras sp* and correlated with the Early Turonian in Israel which started with the *Pseudaspedoceras sp* at 91 Ma (Lewy, 1990). The unconformity surface in the middle part of Maghra El-Hadida Formation at Ataqa Mountain is equivalent to the Middle Turonian Butum Formation at Sinai (Issawi et al., 1999).

SEDIMENTARY FACIES

The Cenomanian and Turonian rocks at Ataqa and Shabrawet mountains are classified into nine sedimentary facies based on the grain size, sedimentary structure, and fossil associations, which reflect their

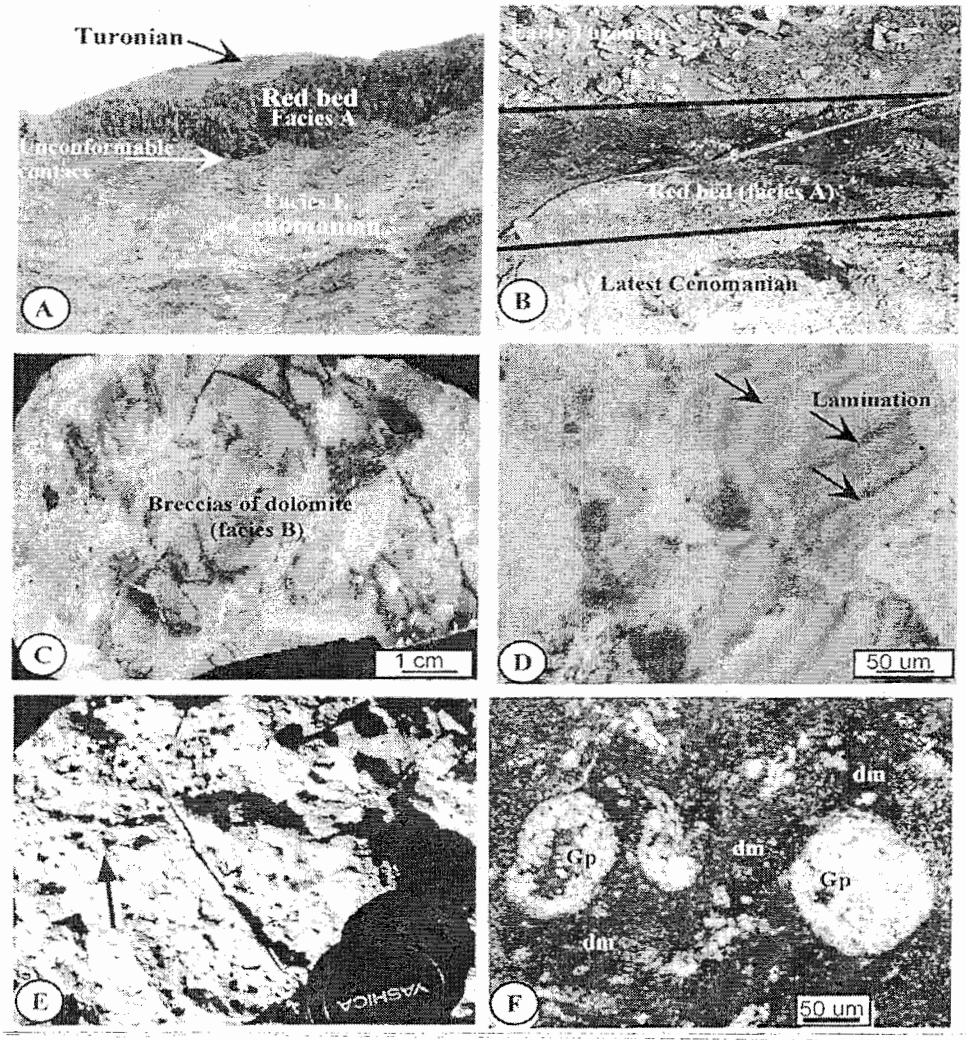

Fig. (5): A) Field photograph shows the red bed unconformably overlies the Latest Cenomanian and gradational underlies the Turonian at Gabal Shabrawet west. B) Field photograph shows the kaolinitic red bed of facies A with red color of iron oxides. C) Field photograph shows the angular fragments of dolomite breccias of facies B and gypsum fand clays in matrix. D) Photomicrograph shows micritic size of dolomite with lamination (see arrows) of facies B. E) Field photograph shows the millimeters size of bird's eye structure (see arrows) in dolomite of facies C. F) Photomicrograph shows the bird's eye filled by gypsum (Gp) in the dolomicrite (dm) of facies C.

depositional environments. These facies are named A through I, and their characters are summarized in Table 2.

1- Facies A (Red Bed)

The red bed of facies A is recorded at the top of the Cenomanian rocks at Gabal Shabrawet (Fig. 5A). Facies A is composed of friable, moderately massive, red clay associated with gypsum nodules and poorly sorted medium to coarse quartz grains. The lower contact of facies A is an irregular erosional surface (Fig. 5B) with reworked fragments from the underlying reddish white clayey dolostone (facies E). The angular fragments are coated by ferruginous iron oxide that shows red color. The red color of facies A is due to the abundance of iron oxides. There is no primary sedimentary structure, and the fossils are absent. The upper contact is gradational to the overlying fenestral dolostone (facies C). This facies occurs only at one level in Gabal Shabrawet. The thickness of facies A ranges from 20 cm to 1 m with average thickness 60 cm and extended a few kilometers laterally. X-Ray diffraction for the bulk samples of red bed shows dominant kaolinite, goethite and quartz minerals. XRD for clay fraction in the red bed reflected mainly kaolinite clay mineral. This type of red bed is similar to the high-lying duricrust (ferricrete) that fall within altitude between 270-300 m above sea level in the Bahariya Oasis (El-Aref et al.1991) due to the old erosion cycle caused by uplifted the Upper Cretaceous-Eocene rocks under humid paleoclimate. The composition of ferricrete is mainly kaolinite, goethite and highly ferrugination (El-Aref et al. 1991). Absence of fossils, high concentration of kaolinitic clay mineral, goethite iron oxides in the red bed and presence of reworked lithic fragments from the underlying formation suggests that the red bed is ferricete reworked origin with period of intensive weathering.

2- Facies B (Laminated Dolostone)

Facies B is composed of red to reddish white, hard, laminated dolomite, and ranges in thickness from 20 to 70 cm. This laminated dolostone at Gabal Shabrawet is underlain by clayey dolostone of facies E with a sharp non-erosional contact and overlain by fenestral dolostone of facies C with a truncated erosional contact. Whereas at Ataqa Mountain, the laminated dolostone (facies B) is overlain by facies D with erosional contact and underlain by facies G with sharp contact. Facies B is characterized by red fragments of laminated dolomite that are ranging from a few millimeters to 5 cm in diameter and the interstice between the

Table (2): Classification of sedimentary facies in Cenomanian-Turonian sedimentary succession at Gabal Shabrawet and Gabal Ataqa.

Facies name	Lithology	Sedimentary structure	Other features	Estimated depositional environment
A	Red bed	No sedimentary structure	Red pigment of iron oxide, nodules of ferricrete and proken fragments reworked from the underlying beds	Intensive weathering
B	Laminated dolomite	Lamination, and evaporite filling pores	Broken fragments of dolomite breccias	Supratridal
C	Fenestral dolomite	Spherical to ovoidal bird's eyes structure filled by evaporites	dolomicrite	Upper intertidal
D	Massive sandstone	Burrows of *Ophiomorpha annulata*	Iron nodules and skeletal grains of phosphorites	Middle shore-face
E	Clayey dolostone	Silty lamination	Sucrosic dolomite with abundance of molluscan fossils and high porosity	Shallow subtidal
F	Sandy dolostone	Burrows of *Thalassinoides suevicus*	Poorly sorted quartz	Shallow subtidal to lower intertidal
G	Fossiliferous limestone	White color and massive beds	Abundance of molluscan fossils, and crinoids	Subtidal zone
H	Foraminiferal limestone.	No sedimentary structure	Globigerinoides and micrite matrix	low energy open marine environment
I	Marlstone	Poorly preserved laminae	Abundance of well preserved molluscous fossils	Subtidal zone

fragments is partially filled with authigenic gypsum and kaolinitic clays (Fig. 5C).

Petrographic examination revealed that the laminated dolomite of facies B is composed of 95% dolomite, and 5% gypsum and reddish brown clays (Fig. 5D). The angular fragments of laminated dolomite breccias and presence of vuges partially filled by gypsum suggests the breccias formed in supratidal flat (Shinn, 1983).

3- Facie C (Fenestral Dolomite)

Facies C is composed of yellowish to grayish white, very hard fenestral dolomite with bird's eye structures (Fig. 5E) with thickness up to 1m. Facies C at Gabal Shabrawet is recorded at two levels, the first level is overlying the tepee structure of facies B with erosional contact and underlying the collapse breccias of facies B with non-erosional contact. The second level of facies C is overlying facies A with gradational contact and underlying the sandy dolostone (facies F) with sharp contact. At Gabal Ataqa, facies C is underlying facies F with sharp contact and overlying facies D with sharp contact. The microscopic examination revealed that this facies is composed of micritic dolomite and bird's eyes filled by gypsum of few millimeters in diameter (Fig. 5F). The bird's eyes are spherical to ovoidal in shape, filled with gypsum that has sharp contact with host dolomite. The presence of bird's eye structures in dolomicrite suggests deposition in peritidal environment, especially in the upper intertidal to supratidal zones (Hardie and Ginsburg, 1977; Park, 1976; Shinn, 1983 and Wanless et al. 1988).

4- Facies D (Massive Sandstone)

Facies D is characterized by yellow to yellowish white, friable to moderately hard, poorly to moderate-sorted, massive, medium to coarse sandstone (Fig. 6A). There is no primary sedimentary structure. Fossils are rare in this facies. Facies D has burrows identified as *Ophiomorpha annulata*, which suggests deposition in middle shore-face (Ksiazkiewicz, 1977). Seilacher (1967) and Kennedy (1975) suggest that *Ophiomorpha* characterizes the intertidal carbonate environment. Thickness of facies D ranges from 1 to 6 m with an average thickness of 3.5 m. At Gabal Ataqa, facies D generally underlies limestone of facies G with a sharp conformable contact and overlies sandy dolostone of facies F (Fig. 4) with an erosional contact. At Gabal Shabrawet, facies D overlies the clayey dolostone of facies E with an erosional contact and underlies limestone of

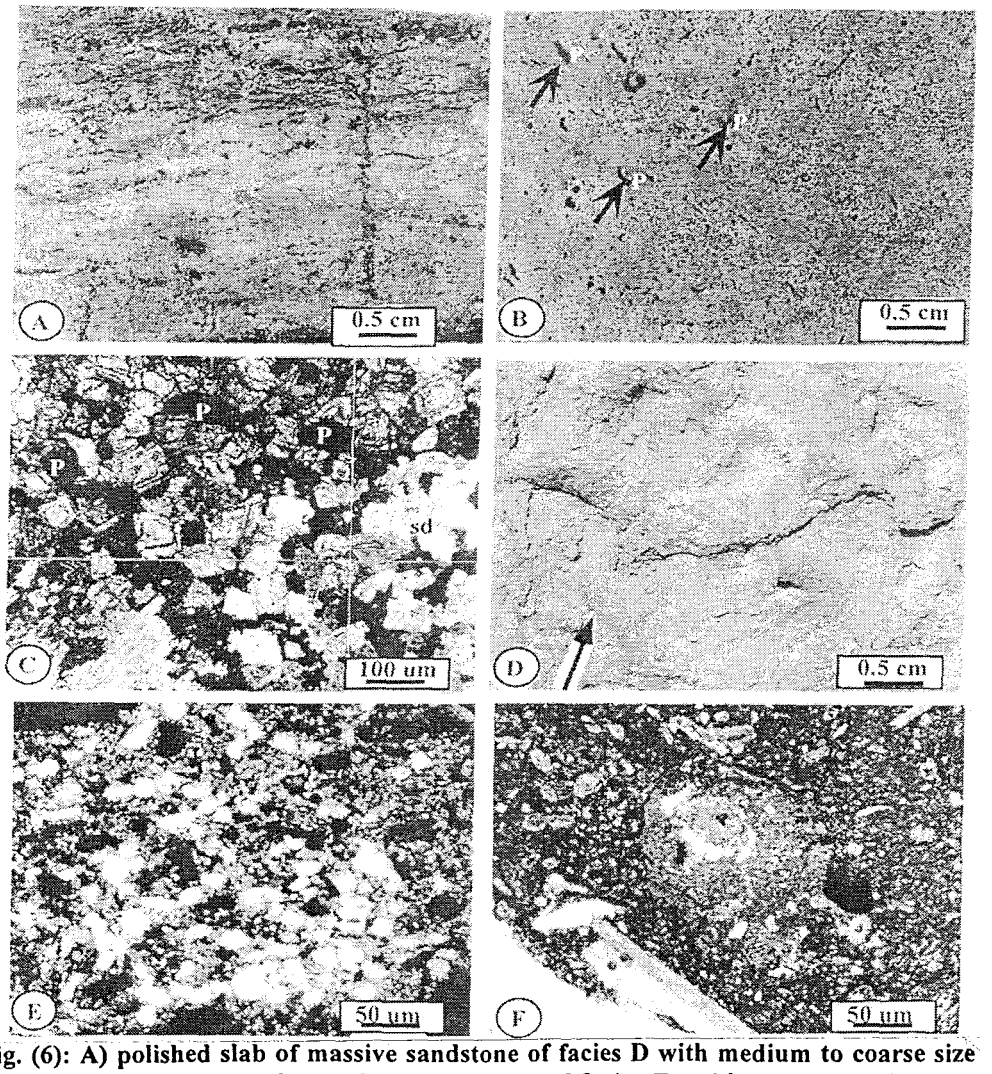

Fig. (6): A) polished slab of massive sandstone of facies D with medium to coarse size grains. B) Polished slab shows clayey dolostone of facies E with empty small vuggy porosity (p). C) Photomicrograph shows the clayey dolostone of facies E is composed of constructive fabrics of sucrosic dolomite (sd) with empty intercrystalline pores (p). D) Field photograph shows sandy dolostone of facies F with burrows *Thalassinoides surevicus* in cylindrical shape (10 cm long and 1cm or less in diatmeter). E) photomicrograph shows sandy dolostone of facies F is composed of very fine dolomite rhombs with fine sand fills the burrows. F) Photomicrograph shows bivalves and echinoides of bioclastic wackestone of facies G.

facies G with a gradational contact. This facies is composed of 85-90 % of medium, poorly sorted, angular to subrounded detrital quartz, 5 % of skeletal phosphatic bone fragments, and 5% of calcite spar with dolomite cement. The presence of *Ophiomorpha annulata* in facies D with poorly sorted quartz and skeletal phosphatic grains support deposition in middle shore face of intertidal environment (Ksiazkiewicz, 1977).

5- Facies E (Clayey Dolostone)

Facies E is characterized by yellow to yellowish brown, porous, moderately hard, limonitic clayey dolostone. This facies contains abundant mollusca remains such as *Exogyra conica, E. africana, Cardita forgemoli* and *Natica* sp. and echinoids such as *Hemiaster cubicus* that suggest inner shelf environment (Emery et al., 1965). The clayey dolostone is intercalated with thin beds of silty claystone, which included in this facies (Fig. 6B) with thickness up to 2m. Facies E is the dominant sedimentary facies in the lower and upper members of the Cenomanian Galala Formation at Gabal Shabrawet and Gabal Ataqa. The lower contact of facies E with the underlying sedimentary facies of G or I is sharp and non-erosional except one erosional contact with the collapse breccias of facies B at Gabal Shabrawet. The upper contact of facies E is an erosional contact with facies D or A. Petrographic examination revealed that the clayey dolostone is composed of 80-85 % idiotopic sucrose crystalline dolomite rhombs of 50-100 um in diameter, 5 % skeletal molluscan and echinoidal particles, 10 % clay matrix with detrital quartz, and 5 % or less of pores partially filled with fine silt (Fig. 6C).

Ruppel (1986), Ruppel and Cander (1988), and Leary and Vogt (1986) studied stacked reservoir cycles of the Upper Ordovician Red River Formation in the Williston basin and described the subtidal dolomitized interval that overlies skeletal and pelletal wackestone and packestone facies with a sharp contact, and underlies supratidal very fine sucrose crystalline dolomite (10-100 μm) with a non-erosional contact. These characters are similar to those of facies E, suggesting subtidal setting facies E. Choquette et al. (1992) studied the pores in shelf dolostones in the Mississippian Burlington-Keokuk Formation and concluded that the sucrosic dolostone is composed of more than 90 % dolomite rhombs of 50-200 μm in size with molds of subtidal fossils indicating that the deposition of sucrose dolomite was in subtidal environment. The clayey dolostone of facies E characterized by relics of subtidal molluscs and echinoide fossils, which is characterized with subtidal undolomitized bioclastic wackestone.

These evidences suggest deposition of facies E in shallow subtidal environment.

6- Facies F (Sandy Dolostone)

Facies F is composed of brownish white to yellow, hard, sandy dolostone with silty lamination, intercalated with thin beds of pale green to gray, friable to moderately hard, silty claystone rich in *Exogrya* sp., *Hemiaster* sp. and *Natica* sp with thickness reach to 0.5 m. Facies F at Gabal Shabrawet have a sharp contact with the overlying facies I and underlying facies C. Facies F at Gabal Ataqa overlies facies C with a sharp contact and underlies facies D with an erosional contact. The basal part of facies F is characterized with horizontal to oblique cylindrical burrows with 5-10 cm long and few centimeters in diameter. Bromley, (1967) identified these cylindrical burrows as *Thalassinoides suevicus* (Fig. 6D). According to Bromley (1967), Kennedy (1970), and Frey and Howard (1990) *Thalassinoides suevicus* represents dwelling structures of predaceous worms in middle shore-face. Petrographic examination revealed that the sandy dolostone is composed of dolomite (75-85 %), detrital quartz (15-20 %), skeletal fragments of molluscs and echinoids (5 %) and yellowish brown clay matrix (5%). Quartz grains are very fine, angular to subrounded, and poorly sorted (Fig. 6E). The presence of silty lamination in sandy dolomite with burrows in the basal part supports deposition in shallow subtidal to lower intertidal environment (Frey and Howard, 1990).

7- Facies G (Fossiliferous Limestone)

Facies G is composed of white to yellowish white, moderately hard, massive limestone with high abundance of bivalves (*Exogyra* sp. *and Natica* sp) and echinoderms (*Hemiaster cubicus*) in living position (Fig. 6F). Facies G is 3 to 6 m thick and overlies marlstone of facies I with a gradual non-erosional contact and overlain by clayey dolostone of facies E with a sharp non-erosional contact. Petrographic examination showed that facies G is composed of 80-90 % micrite, 10-15 % shell fragments, and 5 % calcite spar. The massive limestone is bioclastic wackestone according to the classification of Dunham (1962). Wilson (1975) and Flügel (1982) suggested that the bioclastic wackestone is a variety of limestone deposited in shallow water environment with open circulation close to the wave-base. Subtidal bivalves and echinodermal fossils in the bioclastic wackestone suggest subtidal environment near the wave base.

8- Facies H (Foraminiferal Limestone)

This facies is composed of snow white, massive, moderately hard limestone rich in planktonic foraminifera such as *Globotruncana sigali, G. concavata, G. rensi, G. fornicata, G. imbricata, Globigerinelloides ehrenbergi,* and G. *aspar* and benthic foraminifera such as *Gyroidina girardana, G. depressa, Pyrulinoides acuminata, Faujasina carinata,* and *Palmula rugosa* which suggest open marine environment (Flügel, 1982). The foraminiferal limestone attains a thickness of 10-15 m and is underlain by marlstone of facies J with a sharp non-erosional contact and overlain by the conglomerate of Maghra El-Bahari Formation with an angular unconformity at Gabal Ataqa. Microscopic examination of the foraminiferal limestone showed that it is composed of 85-90 % micrite and 10-15 % foraminiferal fossils (Fig. 7A). Flügel (1982) and Wilson (1975) suggested that the mudstone with globigerinides was deposited in basinal deepwater environment with slow sedimentation. Abundance of foraminiferal fossils in micritic matrix suggests deposition in deep marine environment.

9- Facies I (Marlstone)

Facies I is characterized by yellow to brownish yellow, moderately hard marlstone that is partly laminated with silt. The marlstone contains abundant bivalves such as *Exogyra olisiponesis, E. flabellat* and *Pecten* sp with living position. The marlstone have a thickness ranging from 0.5 to 5 m with average thickness of 2.5 m. Facies I is overlain by facies H with a sharp contact and underlain by facies G with a sharp non-erosional contact (Fig. 7B). Petrographic examination revealed that marlstone of facies I is composed of 90-95 % yellow to yellowish brown matrix of clays and carbonates, 5 % very fine silt, and less than 5% molluscan fossils. Emery et al., (1965) interpreted the molluscan and echinoidal fossils such as *Exogyra olisiponesis, E. flabellate* and *Pecten* sp. At Gabal Ataqa and Gabal Shabrawet as indicative of inner shelf environments. These evidences suggest that Facies J was deposited in low energy subtidal marine environment.

EROSIONAL SURFACES

The erosional surfaces in the Cenomanian-Turonian succession are classified into two main types, 1) ravinement surface (RvS), and 2) subaerial erosion surface (SES). Also there are two minor erosional surfaces in the Cenomanian succession are 1) supratidal-subtidal erosional surface (SSES), and 2) supratidal-intertidal erosion surface (SIES). The

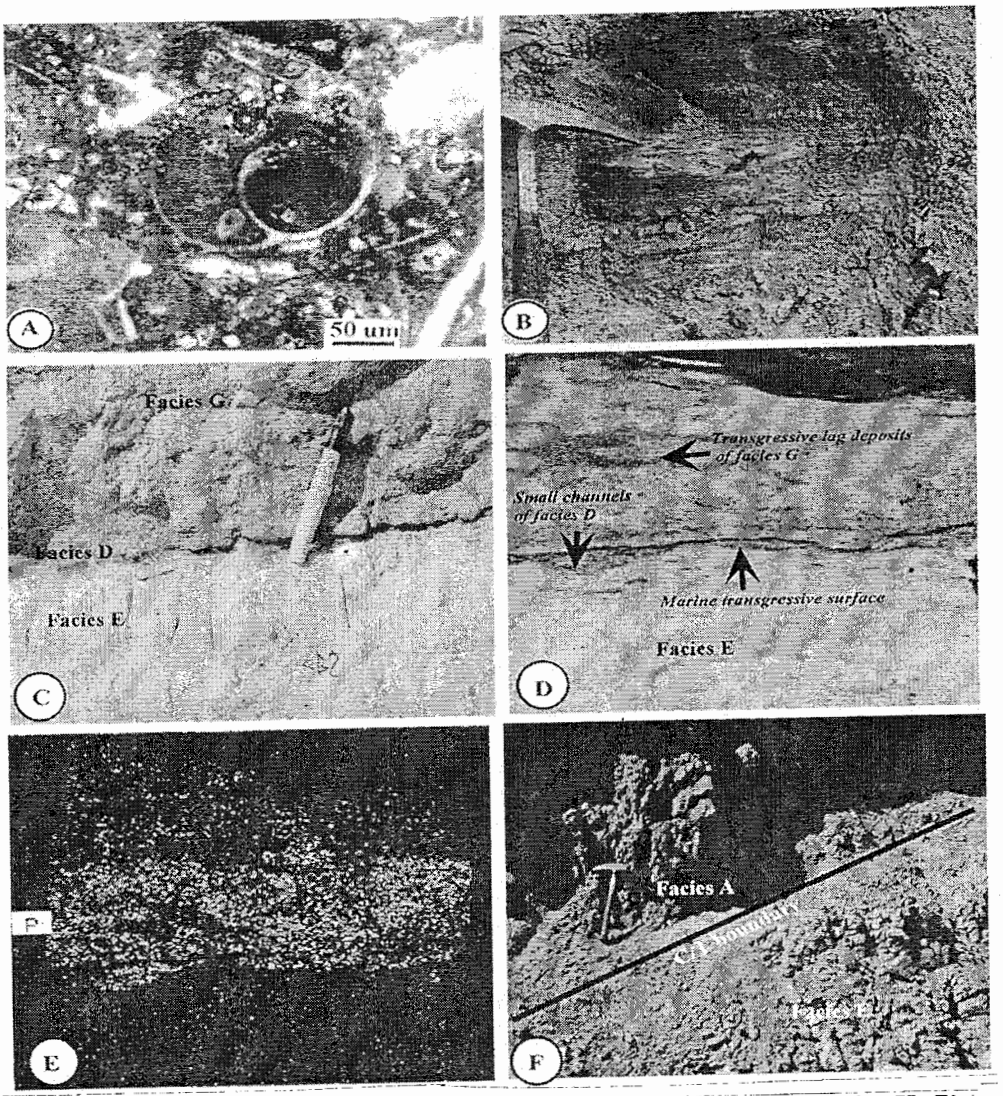

Fig. (7): A) Photomicrograph shows foraminiferal wackestone of facies H. B) Field photograph shows massive yellow marlstone of facies I. C) Ravinement undulated erosional surface. D) Polished slab of last photograph showing the ravinement surface consists of sandstone with phosphatic particles of facies D in small channels and transgressive lag deposits of facies G. E) Chemical scanning of the last polished slab showing the concentration of phosphorus on the concave of ravinement surface. F) Subaerial erosional surface at C/T boundary at Gabal Shabrawet.

classification of these erosional surfaces is based on their geometry, surface morphology, and associated facies below and above the surface.

1-Ravinement surface (RvS)

The ravinement surface is a transgressive surface of erosion that can be formed by wave and current action in the shallow marine environment during marine transgression (Nummedal and Swift 1987). This erosional surface is a surface of sediment transfer from the shoreface to farther seaward during marine transgression and generally overlain by transgressive lag deposits. In this study, this surface is identified as undulated erosional surface that overlies shallow subtidal clayey dolostone of facies E and is overlain by low energy deep subtidal massive limestone of facies G. The ravinment surface is traceable laterally for few kilometers. Ravinement surface characterizes by poorly sorted phosphatic skeletal grains (Figs. 7C&D). Chemical scanning shows high concentration of P_2O_5 in phosphatic grains on the concave part of this surface (Fig. 7E). This erosional surface is identified as a ravinment surface because it represents a trangressive surface bounding the underlying lowstand sediment (facies E) and overlying low energy highstand sediments (facies G), and is characterized by coarse, poorly sorted, phosphatic sand grains that filled the concave parts of the erosional surface. The boulders of limestone in the basal part of massive limestone of facies G are interpreted as the transgressive lag deposits (Fig. 9D).

2- Subaerial Erosional Surface (SES)

The subaerial erosional surface is a surface of subaerial weathering and erosion during periods of lowstand sea level (Nummedal and Swift, 1987). In this study, the subaerial erosional surface is identified as an irregular erosional surface that overlies the shallow subtidal clayey dolostone of facies E and underlies the red kaolinitic clays of facies A. This irregular erosional surface extended laterally for few kilometers and consists of reworked fragments from the underlying rocks of facies E with nodules of calcrete filled the undulated concaves of the surface (Fig. 7F). The red bed above this erosional surface at the Cenomanian-Turonian contact (C/T) suggests ferricrete and reworked origin with a period of intensive weathering. The presence of clayey dolostone of facies E below this erosional surface suggests shallow subtidal zone. This means that this erosional surface may represent a regressive phase followed by a period of subaerial exposure dominated by humid climate and intensive weathering.

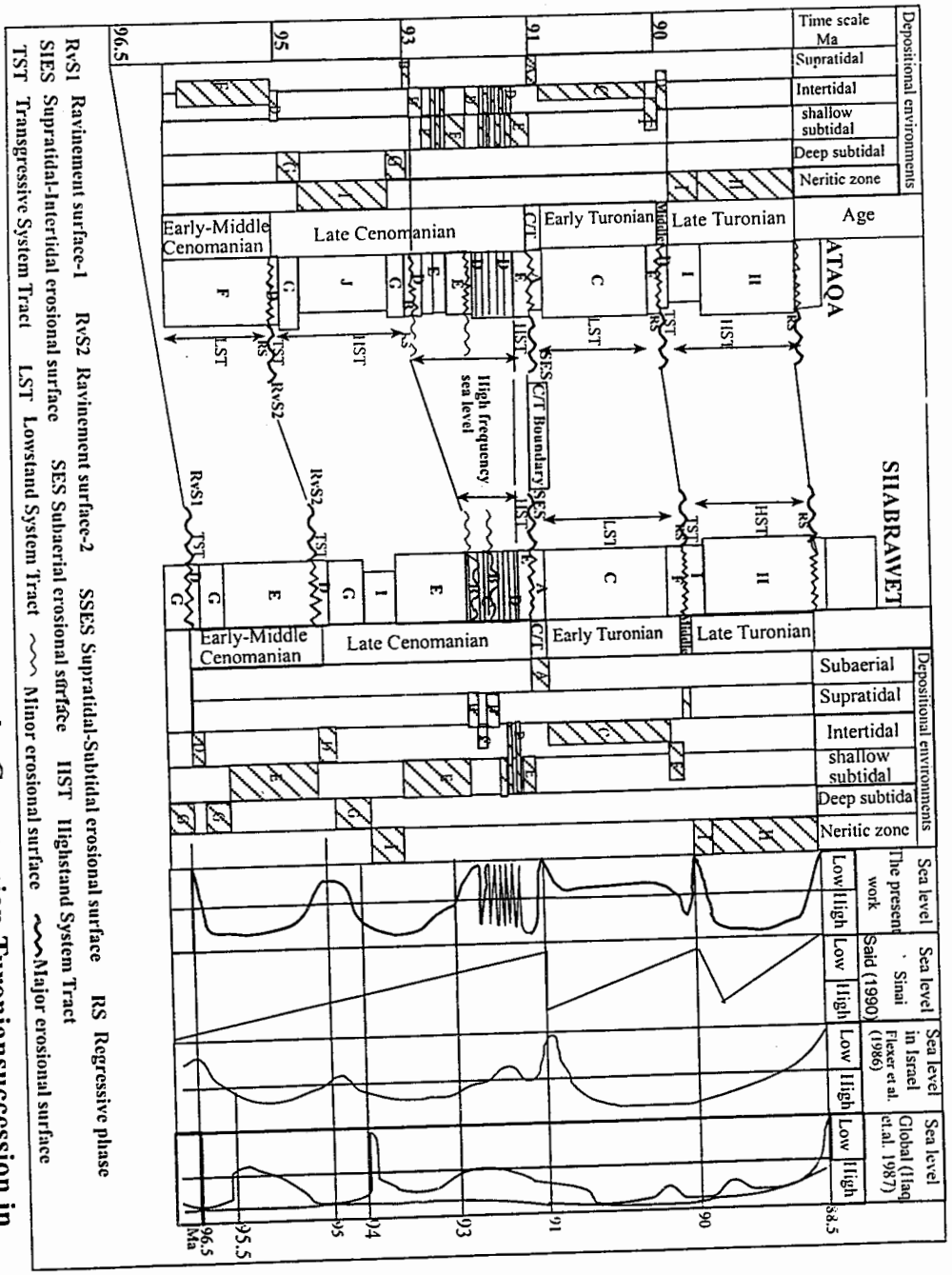

RvS1 Ravinement surface-1 RvS2 Ravinement surface-2 SSES Supratidal-Subtidal erosional surface RS Regressive phase
SIES Supratidal-Intertidal erosional surface SES Subaerial erosional surface IIST Highstand System Tract
TST Transgressive System Tract LST Lowstand System Tract ~~ Minor erosional surface ~~ Major erosional surface

Fig. (8):Reconstructed sea level changess across the Cenomanian-Turonian succession in the studied areas and its correlation with other localities.

This red bed (ferricrete) at C/T boundary may be related to the Cretaceous uplift (El-Aref et al., 1991).

RELATIVE SEA LEVEL CHANGES

Results of detailed analyses of the depositional facies and associated erosional surfaces are shown in figures 3 and 4. All these results used to reconstruct the relative sea level changes during Cenomanian-Turonian at Gabal Shabrawet and Gabal Ataqa (Fig. 8). The reconstructed sea level of Cenomanian-Turonian succession in figure 8 is compared with the sea level of Egypt (Said, 1990), Israel (Flexer, et al., 1986) and the global curve (Haq et al., 1987). So, to understand the reconstructed sea level changes in the present work with other localities (Fig. 8), we will discuss the sea level as follow:- 1) Early-Middle Cenomanian, 2) Late Cenomanian, 3) C/T boundary, and 4) Turonian.

1- Sea level change during Early-Middle Cenomanian

Sea level changes at Gabal Shabrawet and Gabal Ataqa during this time started by marine sea level rise of the Cenomanian above the ravinement surface (RvS1) with gradual rise of sea level during the Early-Middle Cenomanian followed by short-term drop of sea level at the end of the Middle Cenomanian resulting in regressive phase below the ravinement surface (RvS2) (Fig. 8). The ravinement surface (RvS1) represents the Late Ablian/Cenomanian contact (figure 8). This surface (RvS1) in the present sea level curve is equivalent to fall of sea level in the curve of Flexer et al., (1986) in north Israel and response to the global eustatic sea level fluctuations of Haq et al., (1987). The marine transgression of the Cenomanian started at Late Albian and continued up to Late Cenomanian with several minor superimposed sea level fluctuations and short-term sea level falls detected near the Albian/Cenomanian and within the Cenomanian sediments (Figs. 3&4). This short-term recession of sea level at resulted minor break in sedimentation, which may be accompanied by the exposure of paleohighs exhibiting an obvious erosional unconformity (Abed, 1984).

2- Sea level change during Late Cenomanian

The marine transgression started above the ravinement surface (RvS2) with gradual rising of sea level at the early Late Cenomanian. At the middle of Late Cenomanian short term of sea level fall with high frequency of sea level oscillations recorded at Gabal Shabrawet and Gabal Ataqa. The sea level rise occurred during latest Late Cenomanian followed

by abrupt sea level drop at the C/T boundary, which is evidenced by the subaerial erosional surface (SES). The sea level curve of Late Cenomanian at Gabal Shabrawet and Gabal Ataqa resulted maximum amplitude of sea level (HST) in the early of the Late Cenomanian, which is coincided with the curves of Egypt (Said, 1990), Israel (Flexer et al. 1986) and the global (Haq et al., 1987). The high frequency of sea level (Fig. 8) is recorded in the middle Late Cenomanian, which is not recorded in the curves of other localities. The high frequency of sea level changes during the middle Late Cenomanian at Gabal Shabrawet and Ataqa in the present work comprising massive sandstone of facies D (intertidal) intercalated by marlstone of facies E (Subtidal). These oscillations of the transgressive sea caused minor gaps in the carbonate sedimentation evidenced by shoert-term sea level fall. The frequency of the sea level at Gabal Shabrawet and Gabal Ataqa may be caused by orbital driven.

3- C/T boundary

The sea level changes at the late Late Cenomanian is represented by highstand of sea level (subtidal zone of facies E) followed by regressive phase coincide with the subaerial erosional surface (SES) (figure 8). The highstand sea level in the present work is coincided with the global curve of Haq et al. (1987) and Flexer et al. (1986) in Israel. El-Azabi (1998) studied the sequence stratigraphy of the Barremian-Cenomanian succession at Gebel Shabrawet and remarked a Late Cenomanian sequence boundary (type 2 sequence boundary). This boundary is described as paraconformity and marked as distinctive submarine hardground and recorded in the Cenomanian at 93 Ma close to the Cenomanian-Turonian boundary (Haq et al., 1988). The submarine hardground of in the Cenomanian Galala Formation of Gabal Shabrawet (El-Azabi, 1998) is equivalent to the submarine minor erosional surfaces during Late Cenomanian at 93 Ma, below the C/T boundary. The drop of sea level at C/T boundary is followed by period of subaerial exposure with humid climate and intensive weathering represented by the red bed of ferricrete (Fig. 8). The red ferricrete bed above the unconformable contact of C/T boundary is recorded also by Bogoch et al. (1993) as calcrete crust at C/T boundary in in the Galilee of Israel. The calcrete crust at the top of the Sakhin Formation (Cenomanian) in the Galilee, Israel is evidenced by sea level drop at C/T boundary and also presented by Hancock (1989) from the British Chalk, as disconformity surface in the carbonate platform of Provence (Phillip and Airaud-Crumiere 1991).

4- Sea level change during Turonian

The Turonian age started by lowstand of sea level curve, which evidenced by the intertidal fenestral dolomite (facies C) at Gabal Shabrawet and Gabal Ataqa (Fig, 8). The regression at the end of Early Turonian is also demonstrated with fall of sea level, which evidenced by non-fossiliferous sand with iron crust. The Late Turonian is also recognized by rise of sea level. The reconstructed sea level curve during the Turinan age at Gabal Shabrawet and Gabal Ataqa (Fig. 8) is characterized by the following 1) lowstand of sea level at Early Turonian and 2) regressive phase with fall of sea level at Middle Turonian

The lowstand during the Early Turonian is not shown in the sea level curve of Haq et al. (1987) of the curve of Flexer et al. (1986), which may be related to local emergence, which preceded the Early Turonian flood. The drop of sea level at Middle Turonian in the present study is reported as a regressive phase in Central Sinai (Abdel Gawad 1999). This regressive phase of the Middle Turonian in Sinai (Abdel Gawad, 1999) overlies the Early Turonian (*Mammites nodosoides* zone) and underlies the early Late Turonian (*Coliopoceras requienianum* zone of Luger and Groeschke 1989, Kuss 1989 and Abdel Gawad 1999). The drop of sea level during the Middle Turonian should be related to the early pulses of the Syrian Arc Event, which is responsible for this local uplift including the nearby areas of the Arabo-Nubian Shelf (Harris et al. 1984; Flexer et al., 1986). The transgression during the early Late Turonian in the present work (Fig. 8) coincides with the transgression of sea during Late Turonian Wata Formation in North Egypt at Sinai with highstand of sea level (Abdel Gawad, 1999).

The reconstructed sea level curve in the present work demonstrates high frequency of sea level oscillations during the Late Cenomanian and the large drop of sea level at the C/T boundary is also observed.

CONCLUSIONS

The Cenomanian-Turonian succession at Gabal Shabrawet and Gabal Ataqa has been examined for sedimentary facies, fossils content and depositional environments to reconstruct the relative sea level changes. The facies analyses resulted in nine sedimentary facies deposited in shallow marine carbonate plateform. Two main types of erosional surfaces are recognized within the Cenomanian Galala Formation (ravinement surface) and at C/T boundary (subaerial erosional surfaces) to support the reconstructed sea level in the succession. The reconstructed relative sea level changes suggests 1) three short term events of sea level drop during

Late Cenomanian, 2) presence of high frequency sea level oscillations during the Late Cenomanian, 3) abrupt sea level drop at C/T boundary with period of subaerial exposures evidenced by red bed (ferricrete) of the earliest Turonian, 4) renew transgression of sea level during Early Turonian with lowstand of sea level, 5) regressive phase during the Middle Turonian, which is related to the early pulses of the Syrian Arc Event, and 6) transgression during early Late Turonian is coinciding with the transgression of sea during Late Turonian (Wata Formation) in North Sinai with highstand of sea level. These character of the reconstructed sea level changes at Gabal Shabrawet and Ataqa are basically consistent with the sea level from Israel, eustatic sea level of Egypt and the global curve. The high frequency of sea level during the Late Cenomanian may be caused by orbital driven. The lowstand of sea level during the Early Turonian was neither recorded in the global curve nor in nearby (Israel), which may be related to local emergence preceded the Early Turonian.

ACKNOWLEDGEMENTS

Sincere and profound appreciation is expressed to the Japanese Society for the Promotion of sciences (JSPS) for giving me the fellowship to finish my research with Prof. Dr. Ruyji Tada in the University of Tokyo, Department of Earth and Planetary Sciences (EPS). My gratiful appreciation to Prof. Dr. Ryo Matsumoto, the University of Tokyo for his kind help in his lab for IC Mass. My deep thanks to Mrs. Yamamoto, Kato and Goto for their kind helps during my work in EPS lab.

REFERENCES

Abdallah, A.; Adindani, A. and Fahmy, N. (1963): Stratigraphy of lower Mesozoic rocks, western side of Gulf of Suez, Egypt. Geol. Surv. Paper 27, p. 23.

Abdel-Gawad, G. I. (1999): Biostratigraphy and facies of the Turonian in the west-central Sinai, Egypt. Ann. Geol. Surv. Egypt, v. 22, 99-114.

Abed, A. M. (1984): Emergence of Wadi Miyib (central Jordan) during Lower Cenomanian time and its regional tectonic implications. In: The geological evolution of the eastern Mediterranean, by J. E. Dixon and A. H. F. Robertson (eds.). Blackwell Scientific Publi , Oxford, 213-216.

Abdallah, A. M.; Abu Khadra A. M.; Darwish, M. and Helba, A. A. (1988): Geology of Gebel Safariat area, southwest Sinai, Egypt. 26th Ann. Meeting Geol. Soc. Egypt Cairo (Abstract).

Abu Khadra, A. M.; Darwish, M.; El-Azabi, M. and Abdel Fattah, M. A. (1987): Lithostratyigraphy of Upper Cretaceous-Tertiary succession in the Gulf of Suez (southern Galala Plateau), Egypt. Current Research in African Earth Sciences. Matheis & Schandelmeir (eds) Balkema, Rotterdam, 171-176.

Al-Ahwani, M. (1982): Geological and sedimentological studies of Gebel Shabrawet area, Suez Canal District, Egypt. Ann. Geol. Surv. Egypt, v. 12, 305-381.

Arthur, M. A., Schlanger, S. O. and Jenkyns, H. C. (1987): The Cenomanian-Turonian Ocean anoxic event, II. Palaeoceanographic controls on organic matter production and preservation. Geol. Soc. Spec. publ. No. 26, 401-420.

Bartove, Y. and Steinitz, G. (1977): The Judea and Mount Scopus Groups in the Negev and Sinai with trend surface analysis of the thickness data. Isr. J. earth Science., v. 26, 119-148.

Bauer, J.; Marzouk, A. M.; Steuber, T. and Kuss, J. (2001): Lithostratigraphy and biostratigraphy of the Cenomanian-Santonian strata of Sinai, Egypt. Cretaceous Research, 22. 497-526.

Bogoch, R. Buchbinder, B., and Magaritz, M. (1993): Sedimentology and geochemistry of lowstand peritidal lithofacies at the Cenomanian-Turonioan boundary in the Cretaceous carbonate platform of Israel. J. Sed. Research, v. A64, no. 4, 733-740.

Bromley, R. G. (1967): Some observation on burrows of Thalassinidean crustacea in chalk hardgrounds. Journal of the Geological Society of London, 123, 157-182.

Choquette, P. W., Cox, A., and Meyers, W. J. (1992): Characteristics, distribution and origin of porosity in shelf dolostones: Burlington-Keokuk Formation (Mississipean), U.S. Mid-continent. J. sed. Petrol. 62. 167-189.

Darwish, M. (1994): Cenomanian-Turonian sequence stratigraphy, basin evolution and hydrocarbon potentialities of northern Egypt. 2nd int. Conf. Geology of the Arab World, Cairo University. 261-303.

Dunham, R. J. (1962): Classification of casbonate rocks according to depoasitional texture. In: Classification of carbonate rocks. AAPG. Memoir. 1, 108-121.

El-Akkad , S. and Abdallah, A. (1971): Contribution to the geology of Gebel Ataqa area. Ann. Geol. Surv. Egypt, v. 1, 21-42.

El-Aref, M.; El-Dougdoug, A. and Mesaed, A. A. (1991): Landform evolution and formation of ferricrete duricrusts, El-Heiz area, El-Bahariya depression, Western Desert, Egypt. Egypt Geol. J. 34, 1-2, 1-39.

El-Azabi, M. (1998): Facies analysis and paleoenvironmental interpretation of Gebel Shabrawet lower/Middle Cretaceous (Barremian-Cenomanian) succession and its sequence stratigraphic applications, north Eastern Desert, Egypt. Geology of Arab World, v.IV, 643-683.

Emery, K. O.; Merrill, A. S., and Trumbell, J. V. A. (1965): Geology and biology of the sea floor as deduced from simultaneous photographs and samples: Limnol. Oceanog., v. 101, 1-12.

Flexer, A., Rosenfeld, A, Lipson,-Benitah, S. and Honigstein, A. (1986): Relative sea level changes during the Cretaceous in Israel. AAPG, v. 70, no. 11, 1685-1699.

Flugel, E. (1982): Microfacies analyses of limestones. Springer Verlage, Berlin, Heidelburg, New York. Pp. 633.

Frey, R. W., and Howard, J. D. (1990): Trace fossils and depositional sequences in a clastic shelf setting, Upper Cretaceous of Utah. J. Paleont. v. 64, 803-820.

Gale, A. S.; Jenkyns, H. C.; Kennedy, W. J. M. and Corfield, R. (1993): Chemostratigraphy versus biostratigraphy: data from around the Cenomanian-Turonian boundary. J. Geol. Soc. London 150, 29-32.

Hancock, J. M. (1989): Sea level changes in the British rgion during Late Crtaceous: Geologists Association Proceedings, v. 100, 565-594.

Haq, B. U.; Hardenbol, J. and Vail, P. R. (1987): The chronology of fluctuating sea level since the Triassic. Science, 235, 1156-1167.

Haq, B. U.; Hardenbol, J. and Vail, P. R. (1988): Mesozoic and Cenozoic chronostratigraphy and cycles of sea level changes, In: Wilgus, C. K., Posamentier, H. W. Ross, C. A., and Kendall, C. G., eds., Sea level changes: An integrated approach: SEPM Special Publication 42, 71-108.

Hardie, L. A. and Ginsburg, R. N. (1977): Layering: The origin and environmental significance of lamination and thin bedding. In: Sedimentation in moderncarbonate tidal flate of northwest Andros Island (Bahamas). Geol., 22, 50-124.

Harris, P. M.; Frost, S. H.; Seigli, G. A. and Schneidermann, N. (1984): Regional unconformities and depositional cycles, Cretaceous of the Arabian Penninsula. J. S. Schlee, eds.,

interregional unconformities and hydrocarbon accumulation: AAPG Memoir 36, 67-80.

Hart, M. B.; Dodsworth, P.; Ditchfield, P. W.; Daunce, A. M. and Orth, C. J. (1991): The Late Cenomanian event in eastern England. Historical Biology 5, 339-548.

Honigstein, A.; Raab, M. and Rosenfeld, A. (1985): Manual of Cretaceous ostracodes from Israel: Israel Geological Survey Special Publication 5, 1-25.

Issawi, B.; El-Hinnawi, M.; Francis, M. and Mazhar, A. (1999): The Phanerozoic geology of Egypt: A geodynamic approach. The Egyptian Geol. Surv. Special Publ. No. 76, pp. 462.

Issawi, B.; Osman, R.; Yehia, M. and El-deftar, T. (1994): The delineation of Sinai water basins by using lithofacies isopach and structural contour maps. 2nd Conf. Geol. Of Arab World, Cairo Univ. 483-497.

Jarvis, I.; Carson, G. A.; Cooper, M. K. E.; Hart, M. B.; Leary, P. N.; Tocher, D. A.; Horne, D. and Rosenfeld, A. (1988): Microfossils assemblage and the Cenomanian-Turonian (Late Cretaceous) Oceanic Anoxic Event. Cretaceous Research 9, 3-103.

Jenkyns, H. C. (1980): Cretaceous anoxic events: from continents to oceans. J. Geol. Soc. London137, 171-181.

Katz, A. (1971): Zoned dolomite crystals: J. Geol. V. 79, 38-51.

Kennedy, W. J. (1970): Trace fossils in the chalk environments. In Trace fossils. Edited by T. P. Crimes and J. C. Harper. Geological Journal, Special issue 3, 263-282.

Kennedy, W. J. (1975): Trace fossils in carbonate rocks. In the study of trace fossils. Edited by R. W. Frey. Springer Verlage, New York, 377-398.

Kuss, J. (1989): Facies and paleogeographic importance of the pre-rift limestone from NE-Egypt, Sinai, Geol. Redsch., v. 78, no. 2, 487-498.

Ksiazkiewicz, M. (1977): Trace fossils in the flysch of the Polish Carpathians. Paleontologia Polonica, 36, 1-208.

Leary, D. A. and Vogt, J. N. (1986): Diagenesis of the Permian San Andres Formation, Central Basin Platform, West Texas: in Bebout, D. G. and Harris, P. M. eds., Hydrocarbon reservoir studies, San Andreas Formation, Permian Basin, PBS, SEPM Publ., 86, 67-86.

Lewy, Z. (1990): Transgressions, regressions and relative sea level changes on the Cretaceous shelf of Israel and adjacent countries. A

Critical evolution of Cretaceous global sea level correlations. Palaeoceanography, v. 5, no. 4, 619-637.

Lewy, Z. (1996): The approximate position of the Middle-Upper Cenomanian substage boundary in Israel. Israel J. earth science 45, 193-199.

Luger, P. and Groeschke, M. (1989): Late Cretacous ammonites from the wadi Qena area in the Egyptian Eastern Desert. Paleontology, v. 32, 355-407.

Nummedal, D. and Wift, D. J. (1987): Transgressive stratigraphy at sequence bounding unconformities: Some principles derived from Holocene and Cretaceous examples, in Nummedal, D., Pilky, O. H. and Howard, J. D. eds., Sea level fluctuation and coastal evolution: SEPM, special Publ. 41, 241-260.

Orabi, O. H. (1994): Paleoecology of the ostracodal assemblages of the Upper Cretaceous rocks of Wadi Zelica (Gulf of Aqaba and wadi Maghra El-Hadida, Gulf of Suez), Egypt. Delta J. Sci. 18, 115-143.

Park, R. (1976): A note on the significance of lamination stromatolites. Sedimentology, v. 23, 379-393.

Phillip, J. M. and Airaud-Crumiere, C. (1991): The demise of rudist-bearing carbonate platforms at the Cenomanian/Turonian boundary: a global control: Coral Reefs, v. 10, 115-125.

Rosenfeld, A. and Raab, M. (1974): Cenomanian-Turonian ostracodes from the Judea Group in Israel: Israel Geol. Surv. Bull. 62, 1-64.

Ruppel, S. C. (1986): San Andreas facies and porosity distribution Emma field, Andrews Country Texas, in Behout, D. G. Harris, P. M. eds., Hydrocarbon reservoir studies San Andres/Grayburg formations, Permian Basin, PBS, SEPM Spec. Publ. No. 86, 99-103.

Ruppel, S. C. and Cander, H. S. (1988): Dolomitization of shallow water platform carbonates by seawater-seawater derived brines: San Andres Formation, West Texas, in Shukla, V., Baker, P. A. eds., Sedimentology and geochemistry of dolostones, Soc. Econ. Paleontologists and Mineralogists Spec. Publ. 43, 245-262.

Said, R. (1990): Cretaceous paleogeographic maps. In: The geology of Egypt, by R. Said (ed.). Balkema, Rotterdam, 439-449.

Schlanger, S. O. and Jenkyns, H. C. (1976): Cretaceous Oceanic Anoxic Events: causes and consequences: Geologie in Mijnbouw 55, 179-184.

Shinn, E. (1983): Birdeyes fenestrae, shrinkage pores and loferites: A reevaluation. J. Sed. Petrol. v. 53, no. 2, 619-628.

Seilacher, A. (1967): Spuren und fazies im unterkambrium. In O. H. Schindwolf and A. seilacher, Beitrag zur kenntnis des Kambrium in der salt range. Akademie der wissenschaftlen und der literature zu mainz, mathematisch-naturwissenschaften klasse, Abhandlungen, 10, 373-399.

Wanless, H. R.; Tyrrell, K. M.; Tedesco, L. P. and Dravis, J. J. (1988): Tidal flate sedimentationfrom Hurricane kate, caicos platform, British west indies. J. Sed. Petrol. V. 58, no. 4, 724-738.

Weimer, R. J. (1984): relation of unconformities, tectonics and sea level changes, Cretaceous of Western interior, U.S.A. In J. S. Schlee, eds., Interregional unconformities and hydrocarbon accumulation: AAPG memoir 36, 7-35.

Wilson, J. L. (1975): Carbonate facies in geological history. Springer, Berlin. p. 471.

تحليل سحنى لتتابعات السينومانى-التورونى فى منطقة جبل عتاقة وجبل شبراويت، خليج السويس، مصر. تطبيقات لبناء منحنى تغير منسوب سطح البحر

1- د/ محمد محمود أبو الحسن أستاذ الجيولوجيا المساعد - كلية العلوم - جامعة المنوفية
2- أ.د/ روجى تادا أستاذ الجيولوجيا- شعبة علوم الأرض-جامعة طوكيو- اليابان

تتابعات السينومانى-التورونى والمكونة من طبقات كربوناتية و فتاتية فى جبل شبراويت وجبل عتاقة على طول الجانب الغربى لمنطقة خليج السويس تم تقسيم هذه السحن الرسوبية إلى تسعة أنواع ترسبت فى بيئة ترسيبية بحرية ضحلة. تم التعرف على نوعين أساسيين من أسطح التعرية فى تتابعات السينومانى-التورونى 1- سطح تعرية مكشوف لسطح الأرض Subaerial erosional surface على حدود السينومانى-التورونى و 2- سطح تعرية بحرى نتيجة تقدم سطح البحر Ravinement surface على حدود السينومانى السفلى-الأوسط. بناءا على التحليل السحنى و بيئة الترسيب و أسطح التعرية فى منطقة الدراسة تم بناء منحنى تغير منسوب سطح البحر خلال فترة العصر السينومانى-التورونى.

تغير منسوب سطح البحر بالنسبة لمنطقة الدراسة بدا بإرتفاع لمنسوب سطح البحر أثناء فترة السينومانى المبكر والأوسط. إنخفاض تدريجى لمنسوب سطح البحر فى نهاية السينومانى الأوسط. انسينومانى المتأخر تم تقسيمه إلى ثلاث نطاقات زمنية (مبكر و أوسط و متأخر) حسب تغير منسوب سطح البحر كالآتى:-

1- إرتفاع تدريجى لمنسوب سطح البحر أثناء النطاق المبكر للسينومانى المتأخر,

2- إنخفاض تدريجى مع ظهور تذبذب عالى لمنسوب سطح البحر فى النطاق الأوسط للسينومانى المتأخر, 3- إرتفاع تدريجى لمنسوب سطح البحر فى النطاق الأخير للسينومانى المتأخر. إنخفاض مفاجئ لمنسوب سطح البحر عند حدود السينومانى-التورونى. العصر التورونى فى منطقة جبل شبراويت وجبل عتاقة يمثل متكون مغرا الحديدة ويتميز منحنى منسوب سطح البحر فيه بالآتى:-1- إنخفاض منسوب سطح البحر للتورونى المبكر, 2- إنخفاض مفاجئ لمنسوب سطح البحر عند التورونى الأوسط, 3- إرتفاع منسوب سطح البحر للتورونى المتأخر. مما سبق يتضح أن منحنى تغير منسوب سطح البحرللسينومانى-التورونى لمنطقة الدراسة يتميز برؤية واضحة وإضافة جديدة لتذبذب منسوب سطح البحر خلال السينومانى الأوسط والمتأخر.